J|A|C|S
ARTICLES
Published on Web 12/06/2006

Microsolvation Effects on the Excited-State Dynamics of Protonated Tryptophan

Sébastien R. Mercier,[†] Oleg V. Boyarkin,*[,†] Anthi Kamariotis,[†] Matteo Guglielmi,[‡] Ivano Tavernelli,[‡] Michele Cascella,[‡] Ursula Rothlisberger,[‡] and Thomas R. Rizzo*[,†]

Contribution from the Institute of Chemical Sciences and Engineering, École Polytechnique Fédérale de Lausanne, CH-1015 Lausanne, Switzerland

Received August 17, 2006; E-mail: thomas.rizzo@epfl.ch; oleg.boiarkin@epfl.ch

Abstract: To better understand the complex photophysics of the amino acid tryptophan, which is widely used as a probe of protein structure and dynamics, we have measured electronic spectra of protonated, gas-phase tryptophan solvated with a controlled number of water molecules and cooled to ~10 K. We observe that, even at this temperature, the bare molecule exhibits a broad electronic spectrum, implying ultrafast, nonradiative decay of the excited state. Surprisingly, the addition of two water molecules sufficiently lengthens the excited-state lifetime that we obtain a fully vibrationally resolved electronic spectrum. Quantum chemical calculations at the RI-CC2/aug-cc-pVDZ level, together with TDDFT/pw based first-principles MD simulations of the excited-state dynamics, clearly demonstrate how interactions with water destabilize the photodissociative states and increase the excited-state lifetime.

Introduction

Despite the wide use of the amino acid tryptophan as a spectroscopic probe of protein structure and dynamics, its photophysics is not completely understood, particularly its nonexponential fluorescence decay.[1−5] While it seems clear that conformational heterogeneity plays an important role in the time-resolved fluorescence observed from electronically excited tryptophan within proteins,[2,3,6] understanding how different local environments affect the excited-state lifetime is essential for interpretation of the dynamics.[7,8] One of the most important processes that influences this lifetime is charge transfer from the indole ring of tryptophan to a nearby electrophile, a process that is highly sensitive to the local electrostatic environment.[1,2,7,9] The local electric field results from the presence of charged groups in the vicinity of the chromophore as well as any water or polar groups that may solvate the charges and moderate their influence. To better understand the excited-state dynamics of tryptophan embedded in proteins and interpret its use as a probe, it would be helpful to have a molecular level understanding of such effects.

Spectroscopic studies of isolated tryptophan can shed light on its behavior in the more complex environment of a protein. For example, spectroscopic experiments on neutral, gas-phase tryptophan in the cold environment of a supersonic molecular beam have identified individual stable conformers of the isolated molecule,[10] providing support for the rotamer model of tryptophan fluorescence decay in proteins.[5] One way to unravel the effects of the local electric field and solvent on the excited-state lifetime is to investigate protonated tryptophan[11,12] or small tryptophan-containing peptides. Toward this end, we have recently developed a new method to study the spectroscopy and dynamics of cold, biomolecular ions and have applied this approach to investigate the electronic spectroscopy of protonated tryptophan and tyrosine.[13] The spectral features of protonated tyrosine become perfectly sharp upon cooling in the trap, exhibiting a width of only 2.7 cm^{-1}, which arises largely from the rotational contour of a given band. The nearly complete absence of hot bands to the low-energy side of the band origin indicates that the vibrational temperature is approximately 10 K. Under the same conditions, the spectral features of cold, protonated tryptophan exhibit widths > 300 cm^{-1}, suggesting that the excited-state lifetime of this molecule is short.[13] This is qualitatively consistent with time-resolved, pump−probe studies of the same species, which reveal a fast (380 fs) excited-state decay in protonated tryptophan that extends to 22 ps in protonated tyrosine.[14]

[†] Laboratoire de Chimie Physique Moléculaire.
[‡] Laboratoire de Chimie et Biochimie Computationelle.

(1) Liu, T. Q.; Callis, P. R.; Hesp, B. H.; Broos, J.; de Groot, M.; Buma, W. J. *Biophys. J.* **2005**, *88*, 372A-372A.
(2) Callis, P. R.; Vivian, J. T. *Chem. Phys. Lett.* **2003**, *369*, 409−414.
(3) Lakowicz, J. R. *Photochem. Photobiol.* **2000**, *72*, 421−437.
(4) Petrich, J. W.; Chang, M. C.; McDonald, D. B.; Fleming, G. R. *J. Am. Chem. Soc.* **1983**, *105*, 3824−3832.
(5) Szabo, A. G.; Rayner, D. M. *J. Am. Chem. Soc.* **1980**, *102*, 554−563.
(6) Engelborghs, Y. *J. Fluoresc.* **2003**, *13*, 9−16.
(7) Marquezin, C. A.; Hirata, L. Y.; Juliano, L.; Ito, A. S. *Biopolymers* **2003**, *71*, 569−576.
(8) Engelborghs, Y. *Spectrochim. Acta A* **2001**, *57*, 2255−2270.
(9) Dedonder-Lardeux, C.; Jouvet, C.; Perun, S.; Sobolewski, A. L. *Phys. Chem. Chem. Phys.* **2003**, *5*, 5118−5126.
(10) Rizzo, T. R.; Park, Y. D.; Peteanu, L. A.; Levy, D. H. *J. Chem. Phys.* **1986**, *84*, 2534−2541.
(11) Nolting, D.; Marian, C.; Weinkauf, R. *Phys. Chem. Chem. Phys.* **2004**, *6*, 2633−2640.
(12) Talbot, F. O.; Tabarin, T.; Antoine, R.; Broyer, M.; Dugourd, P. *J. Chem. Phys.* **2005**, *122*, 74310−74310.
(13) Boyarkin, O. V.; Mercier, S. R.; Kamariotis, A.; Rizzo, T. R. *J. Am. Chem. Soc.* **2006**, *128*, 2816.
(14) Kang, H.; Jouvet, C.; Dedonder-Lardeux, C.; Martrenchard, S.; Gregoire, G.; Desfrancois, C.; Schermann, J. P.; Barat, M.; Fayeton, J. A. *Phys. Chem. Chem. Phys.* **2005**, *7*, 394−398.

10.1021/ja065980n CCC: $33.50

The spectrum of cold, protonated tryptophan[13] and the short excited-state lifetime that it implies are in stark contrast to those of the neutral species, which exhibits a fully resolved rovibronic spectrum[10] and an excited-state lifetime of 10−13 ns in the gas phase.[15] That protonated, gas-phase tryptophan has a shorter lifetime than that of the neutral form should not be entirely surprising; pH dependent studies of tryptophan fluorescence in solution show the same trend with decreasing pH as the protonated form of the amino acid is favored,[7] although not nearly to the same degree. However, the simple fact that in solution the excited state of protonated tryptophan still lives long enough to fluoresce while in the isolated molecule it does not is contrary to the normal expectation that quenching should be much faster in liquids.

We report here electronic spectra of cold, protonated, gas-phase tryptophan complexed with a controlled number of water molecules together with RI-CC2 and TDDFT calculations in combination with TDDFT-based molecular dynamics simulations of the excited-state dynamics. As described below, the addition of only a few water molecules dramatically lengthens the excited-state lifetime, and our simulations reveal the detailed mechanism of this phenomenon.

Experimental Approach

Our basic experimental approach is to generate closed-shell ions in the gas phase using electrospray, select only those of a particular mass-to-charge ratio (*m*/z), and trap them in a low-temperature ion trap.[13] We then excite the trapped ions with a UV laser pulse and measure the charged fragments that result when some fraction of the excited ions dissociate. We generate a spectrum by monitoring the number of fragment ions of a particular mass-to-charge ratio (*m*/z) as a function of the laser wavenumber. If the molecules remain in the excited state for a sufficient period of time, the spectral features will be sharp, while if fast nonradiative processes occur, the spectral lines will be broadened according to the time−energy uncertainty principle. The spectral features we observe thus provide a rigorous lower limit to the lifetime of the molecule in the excited state.

We produce protonated amino acids as well as their water-containing clusters by nanoelectrospray from a 2×10^{-4} M solution in 50/50 water−methanol with 0.2% of acetic acid added to favor the protonated form of the molecule. We sample the electrospray plume through a glass capillary with metalized ends and collect the ions in an RF-only hexapole trap. After a 48 ms collection time, we pulse the ions out of the hexapole, select a particular mass in a first quadrupole mass spectrometer, bend them 90° with a static quadrupole, and guide them into the 22-pole ion trap,[16−18] which is mounted on a closed cycle refrigerator and maintained at 6 K. We inject a pulse of helium into the trap, giving it sufficient time to equilibrate to the temperature of the trap housing before the arrival of the approaching ion packet. After a 40 ms delay, an ultraviolet laser pulse is sent through the trap, exciting the ions via an electronic transition in the region of 35 000 cm^{-1}. Parent and photofragment ions are released from the trap and passed through an analyzing quadrupole before being detected and counted. The trapping cycle is repeated 20 times per second, while the laser fires at a 10 Hz repetition rate. The parent ion signal recorded between laser shots is used to normalize the data, removing slow fluctuations in the nanospray source. Ultraviolet laser pulses of an ∼5 ns duration are generated by frequency doubling a Nd:YAG pumped dye laser using a beta barium borate (BBO) crystal. Typical UV pulse energy is 10 mJ.

Computational Details

In order to determine the most probable low-energy structures for both bare and solvated $TrpH^+$, we have performed classical MD simulations with the AMBER/parm96 force field[19] at 300 K, a temperature that allows for essentially complete exploration of the conformational space of this system. We find that the conformational space of $TrpH^+$ can be reduced to the orientation of two dihedral angles around the $C-C_\alpha-C_\beta-C_\gamma$ (ϕ_1) and the $C_\alpha-C_\beta-C_\gamma-C_{\delta1}$ (ϕ_2) bonds, as the other structural parameters relax on very short time scales. Using this information, we have then sampled the free energy surface via metadynamics/MD[20] at the experimental temperature of the ion trap (∼10 K), along the relevant degrees of freedom of the system.

For the main species obtained from MD, we have calculated vertical excitations at both TDDFT/B3LYP and single-point second-order approximate coupled-cluster model (CC2)[21] levels. B3LYP calculations are performed using the Gaussian03 code,[22] and CC2 calculations are done using the TURBOMOLE 5.8 code[23] within the resolution-of-the-identity (RI) approximation for the evaluation of the electron-repulsion integrals (RI-CC2).[24] Both TDDFT/B3LYP and RI-CC2 calculations use aug-cc-pVDZ basis sets.[25] We have also performed nonadiabatic excited-state dynamics within time-dependent density functional theory (TDDFT) in the adiabatic (ALDA) approximation.[26] All ground state (DFT) and excited state (TDDFT) MD simulations are carried out with the CPMD code.[27] We use soft norm-conserving nonlocal Troullier−Martins pseudopotentials[28] and a 70 Ry energy cutoff for the plane wave expansion of the wave functions. The inherent periodicity in the plane wave calculations is circumvented by solving Poisson's equation for nonperiodic boundary conditions.[29] We use a cubic cell of size 17 Å for the bare protonated tryptophan ($TrpH^+$) and 23 Å for the doubly solvated species ($TrpH^+(H_2O)_2$). Since the use of hybrid functionals is prohibitive within a plane wave based scheme, excited-state dynamics are run with a GGA (PBE)[30] functional. The main difference between B3LYP and PBE descriptions consists in a constant shift of all calculated transitions to lower excitation energies by ca. 0.6−0.7 eV (when using PBE). The results of DFT/PBE TDDFT dynamics are validated by RI-CC2 calculations at different geometries along the MD trajectory. Our implementation of the TDDFT energies and forces[31] makes use of the Tamm−Dancoff approximation (TDA).[32] Surface crossing probabilities are evaluated by the Landau−Zener semiclassical approach.[33] All energies and gradients are converged to a maximum deviation of 10^{-7} au. A time integration step of 15 au (0.36 fs) is used for the ground state simulations, while for the TDDFT MD runs it is reduced to 4 au (0.10 fs). Oscillator strengths are computed according

(15) Philips, L. A.; Webb, S. P.; Martinez, S. J.; Fleming, G. R.; Levy, D. H. *J. Am. Chem. Soc.* **1988**, *110*, 1352−1355.
(16) Gerlich, D. *Adv. Chem. Phys.* **1992**, *82*, 1−176.
(17) Schlemmer, S.; Kuhn, T.; Lescop, E.; Gerlich, D. *Int. J. Mass Spectrom.* **1999**, *187*, 589−602.
(18) Schlemmer, S.; Lescop, E.; von Richthofen, J.; Gerlich, D.; Smith, M. A. *J. Chem. Phys.* **2002**, *117*, 2068−2075.
(19) Cornell, W. D.; Cieplak, P.; Bayly, C. I.; Gould, I. R.; Merz, K. M.; Ferguson, D. M.; Spellmeyer, D. C.; Fox, T.; Caldwell, J. W.; Kollman, P. A. *J. Am. Chem. Soc.* **1995**, *117*, 5179−5197.
(20) Laio, A.; Parrinello, M. *Proc. Natl. Acad. Sci. U.S.A.* **2002**, *99*, 12562−12566.
(21) Christiansen, O.; Koch, H.; Jorgensen, P. *Chem. Phys. Lett.* **1995**, *243*, 409−418.
(22) Frisch, M. J.; et al. *GAUSSIAN03*, revision C.02; Gaussian Inc.: Wallingford, CT, 2004.
(23) Ahlrichs, R.; Bar, M.; Haser, M.; Horn, H.; Kolmel, C. *Chem. Phys. Lett.* **1989**, *162*, 165−169.
(24) Weigend, F.; Haser, M.; Patzelt, H.; Ahlrichs, R. *Chem. Phys. Lett.* **1998**, *294*, 143−152.
(25) Woon, D. E.; Dunning, T. H. *J. Chem. Phys.* **1993**, *98*, 1358−1371.
(26) Runge, E.; Gross, E. K. U. *Phys. Rev. Lett.* **1984**, *52*, 997−1000.
(27) *CPMD V3.9*; Copyright IBM Corp 1990−2004, Copyright MPI fuer Festkoerperforschung Stuttgart 1997−2001.
(28) Troullier, N.; Martins, J. L. *Phys. Rev. B* **1991**, *43*, 1993−2006.
(29) Martyna, G. J.; Tuckerman, M. E. *J. Chem. Phys.* **1999**, *110*, 2810−2821.
(30) Perdew, J. P.; Burke, K.; Ernzerhof, M. *Phys. Rev. Lett.* **1996**, *77*, 3865−3868.
(31) Hutter, J. *J. Chem. Phys.* **2003**, *118*, 3928−3934.
(32) Hirata, S.; Head-Gordon, M. *Chem. Phys. Lett.* **1999**, *314*, 291−299.
(33) Wynne, K.; Hochstrasser, R. M. Coherence and adiabaticity in ultrafast electron transfer. In *Electron Transfer-from Isolated Molecules to Biomolecules, Pt 2*, 1999; Vol. 107, pp 263−309.

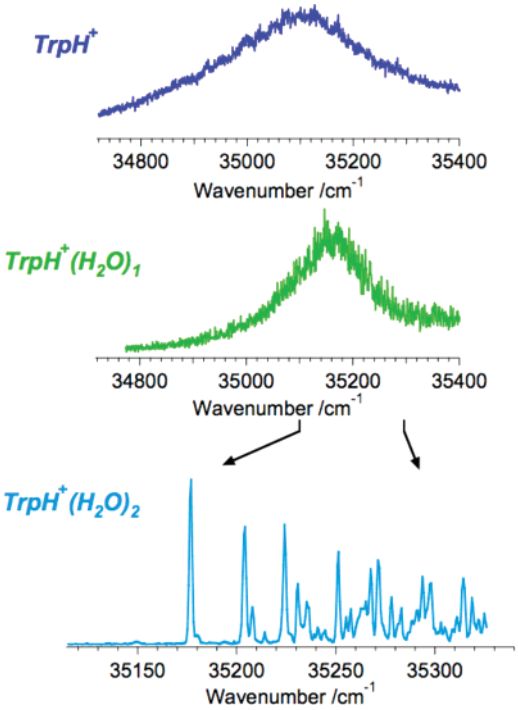

Figure 1. Electronic photofragment action spectrum of protonated tryptophan with 0, 1, and 2 attached water molecules.

to Bernasconi et al.[34] Ground state and excited-state simulations are carried out using Born−Oppenheimer MD.

Results and Discussion

Figure 1 shows the electronic spectrum of protonated tryptophan with 0, 1, and 2 water molecules attached. The broad overall band observed for the bare, protonated tryptophan (top panel) becomes slightly narrower when one water molecule is added but then becomes dramatically sharper upon addition of the second, implying a substantial lengthening of the excited-state lifetime. The features in the spectrum of $TrpH^+(H_2O)_2$ have a similar line width as those of bare, cold, protonated tyrosine.[13] Preliminary assignment of the $TrpH^+(H_2O)_2$ spectrum based upon infrared hole burning studies[35] reveals that one predominant conformer gives rise to the majority of the observed spectral features, which can be assigned to vibrational progressions of several low-frequency vibrations.

While spectral simplification is the opposite of what one typically observes when bare molecules are put in solution, there have been several examples of excited-state lifetime lengthening in gas-phase hydrogen-bonded clusters.[36−39] In these cases, the presence of solvent molecules are proposed to shift different electronic states relative to one another in such a way as to block fast nonradiative decay channels. Our calculations based on single-point RI-CC2 and TDDFT molecular dynamics confirm this general interpretation in the case of protonated tryptophan and reveal the detailed mechanism of the dramatic lifetime lengthening upon solvation.

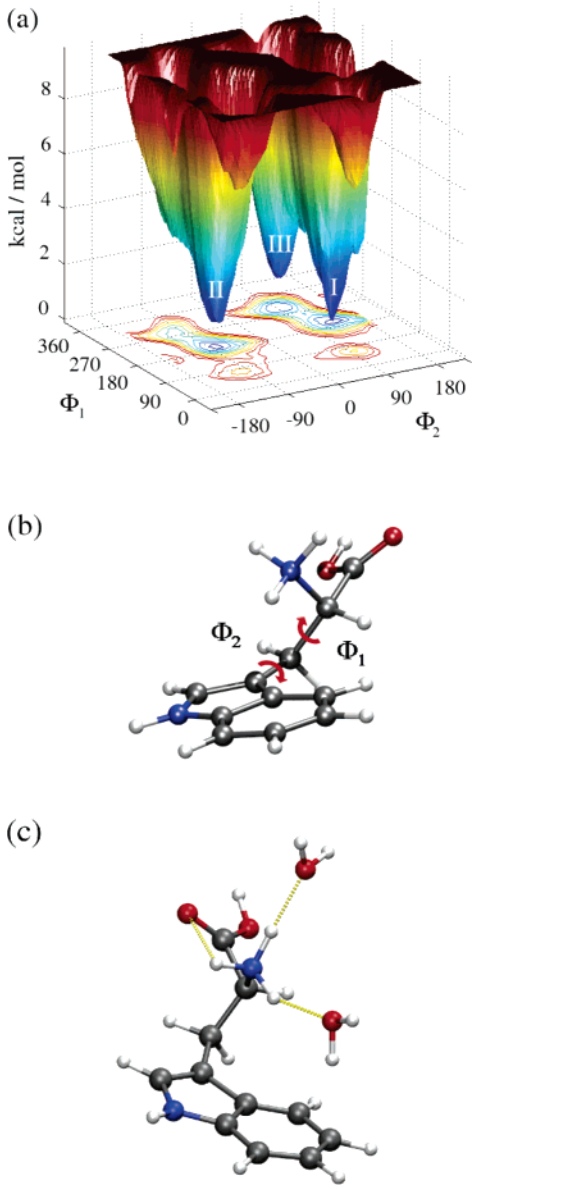

Figure 2. (a) Metadynamics free energy landscape in the (ϕ_1,ϕ_2) subspace for $TrpH^+$ at 10 K. The free-energy scale goes from deep blue (0 kcal/mol) to red (8 kcal/mol). (b) Dominant configurations for $TrpH^+$ (corresponding to minimum I in (a)); and (c) $TrpH(H_2O)_2^+$, as obtained by MD.

The computed free energy landscapes defined by (ϕ_1,ϕ_2) at both 10 K and 300 K show the presence of two possible orientations of the main chain of $TrpH^+$ with respect to the plane of the indole ring ("up" and "down" configurations, hereafter; Figure 2a, labels I and II). Minima I and II are separated by a free energy barrier of ∼7.5 kcal/mol at 10 K. The most probable configuration ("up") shows one deep and one shallow minimum (Figure 2a, labels I, III), separated by a small barrier of ∼2.4 kcal/mol. Assuming that the cooling process in the ion trap is slow enough to allow interconversion between these two minima, only the configuration corresponding to the deeper of the two (shown in Figure 2b) should remain significantly populated at 10 K. The relative energy differences among structures I−II−III ($E_{II}-E_I$ ∼0.3 kcal/mol, $E_{III}-E_{II}$ ∼0.4 kcal/mol) have been confirmed by calculations at the DFT/PBE level within ≤0.1 kcal/mol.

(34) Bernasconi, L.; Sprik, M.; Hutter, J. *J. Chem. Phys.* **2003**, *119*, 12417−12431.
(35) Mercier, S. R.; Stearns, J.; Guidi, M.; Boyarkin, O. V.; Rizzo, T. R. To be published.
(36) Felker, P. M.; Zewail, A. H. *Chem. Phys. Lett.* **1983**, *94*, 454−460.
(37) Hager, J.; Wallace, S. C. *J. Phys. Chem.* **1985**, *89*, 3833−3841.
(38) Sur, A.; Johnson, P. M. *J. Chem. Phys.* **1986**, *84*, 1206−1209.
(39) Mitsui, M.; Ohshima, Y.; Kajimoto, O. *J. Phys. Chem. A* **2000**, *104*, 8660−8670.

Table 1. Five Lowest Vertical Excitation Energies for $TrpH^+$ With Different Methods

excited-state character	RI-CC2 [eV] (smaller basis set)[a]	RI-CC2 [eV] (larger basis set)[b]	B3LYP [eV][b]
$\pi\sigma^*$	4.64	4.46	4.28
$\pi\pi^*$	4.92	4.80	4.71
$\pi\pi^*$	5.18	5.01	4.73
$\pi\pi^*$CO (dark)	>**5.0**	>**5.0**	3.43
$\pi\pi^*$CO (dark)	>**5.0**	>**5.0**	3.89

[a] With aug-cc-pVDZ on O, N atoms, and cc-pVDZ on H,C. [b] With aug-cc-pVDZ on all atoms. The character of the excited states in the first column refers to their largest orbital component.

Simulations of $TrpH^+(H_2O)_2$ reveal that the (ϕ_1,ϕ_2) space has the same topology as that for bare $TrpH^+$. At 300 K, both water molecules always remain directly H-bonded to the NH_3^+ group, showing no preference for other possible locations. For the "up" configuration, annealing to low temperature invariably freezes the two water molecules in the geometry shown in Figure 2c.

Calculations of the vibrational spectra at the DFT/PBE level predict a split in the asymmetric stretch frequencies of the two water molecules of approximately 32 cm^{-1} and 25 cm^{-1} for the "up" and "down" configurations, respectively, in good agreement with our IR hole burning measurements that reveal a difference of 37 cm^{-1} and 20 cm^{-1} for the major and minor conformers.[35] This result supports the assignment of the structure in Figure 2c to the primary conformer observed in our spectra. Note that other higher energy local minima structures found at 300 K give a splitting of less than 12 cm^{-1} for the same antisymmetric stretch bands, also in agreement with our experiments.[35]

Table 1 reports the vertical excitation energies at the equilibrium geometry of bare $TrpH^+$ obtained by DFT and RI-CC2 calculations. As previously discussed in the literature,[36] the calculated excitation spectra for the few lowest optically allowed excitations in the two methods are very similar in terms of both transition energies and the character of the wavefunction. The first optically accessible state lies at 4.28 eV within TDDFT/B3LYP and at 4.46 eV within RI-CC2 calculations (experimental value, 4.35 eV). The TDDFT/B3LYP transition involves the promotion of one electron from the π system on the indole ring to a mixture of σ^*_{N-H} (57%), $\sigma^*_{C\alpha-N}$ (6%), indole π^* (19%), and carboxyl π_{CO}^* (8%) orbitals. The corresponding RI-CC2/aug-cc-pVDZ vertical excitation leads to a similar mixture with percentages: $\sigma^*_{N-H} + \sigma^*_{C\alpha-N}$ (67%), indole π^* (10%), and π^*_{CO} (6%) (see Supporting Information). The precise relative contribution of these three components is strongly geometry dependent (Figure 3a) and, for the RI-CC2 calculations, basis set dependent. At the vertical excitation from the equilibrium geometry, the σ^*_{N-H} contribution is the most significant, in agreement with other recent RI-CC2 calculations.[40] The only difference between RI-CC2 and TDDFT/B3LYP transitions at lower energy is associated with the well-known failure of TDDFT for charge-transfer states,[41,42] which leads to the artificial lowering of two "dark" π^*_{CO} states. However, as previously pointed out[40] and further confirmed by our TDDFT dynamics calculations, these states do not affect the photophysics of this system.

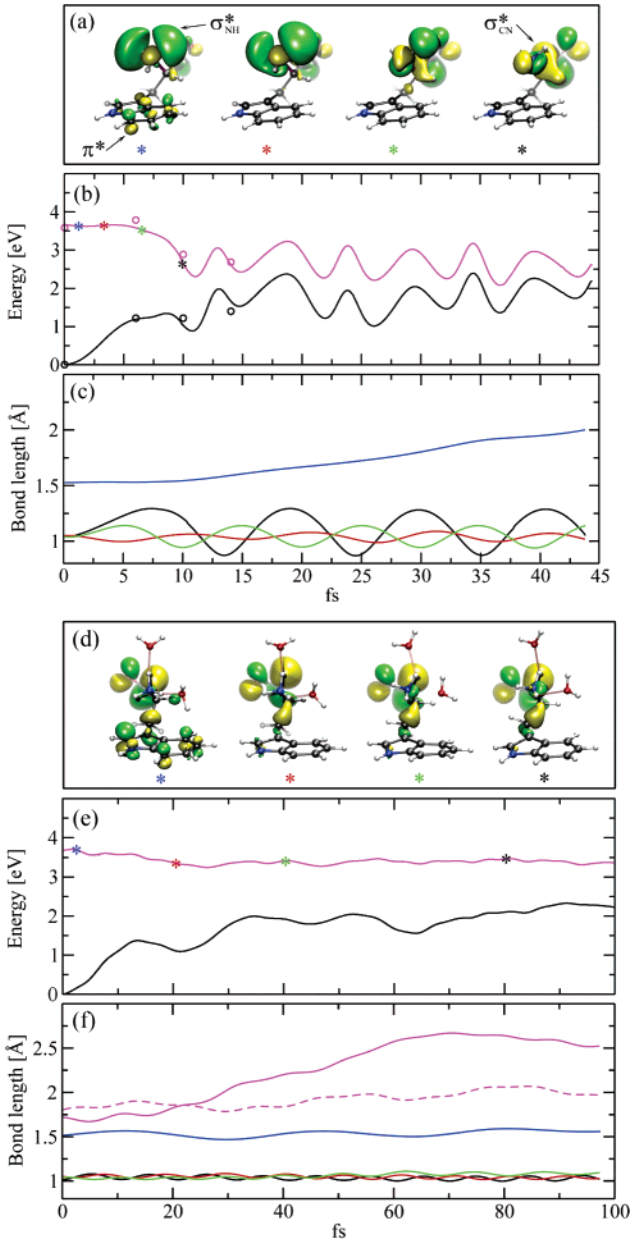

Figure 3. Time evolution of photoexcited $TrpH^+$ (a−c) and $TrpH(H_2O)_2^+$ (d−f). (a/d) Dominant Kohn−Sham orbital contributions to the electronic excited state during TDDFT dynamics at different times. (b/e) Ground and running excited-state energies along the TDDFT dynamics run. The black line shows the ground state energy, and the magenta line, the running diabatic state. The asterisks correspond to the positions where respective snapshots of the orbitals in (a−d) are taken. (c/f) N−H (black, red, and green lines) and C_a−N (blue line) bond lengths, and H_2NH---OH_2 distances (magenta lines) during TDDFT dynamics. In panel (b) black and magenta circles correspond to RI-CC2 energies computed at the corresponding geometries. To facilitate comparison, RI-CC2 excited-state energies are shifted down by a constant amount in order to best match the TDDFT curve.

Figures 3b−c display the time evolution of the $TrpH^+$ system upon vertical excitation to the first photoaccessible state obtained from TDDFT dynamics. During the initial fast relaxation phase (10 fs) along this diabatic state, the σ^*_{N-H} and π^* contributions decrease progressively, while the C_α−N antibonding character increases, as depicted in Figure 3a. These rapid changes in the electronic state induce major structural alterations. In fact, initial stretching of one N−H bond (t < 7.5 fs) is followed by elongation of the C_α−N bond that leads to dissociation of the

(40) Gregoire, G.; Jouvet, C.; Dedonder, C.; Sobolewski, A. L. *Chem. Phys.* **2006**, *324*, 398−404.
(41) Dreuw, A.; Weisman, J. L.; Head-Gordon, M. *J. Chem. Phys.* **2003**, *119*, 2943−2946.
(42) Dreuw, A.; Head-Gordon, M. *J. Am. Chem. Soc.* **2004**, *126*, 4007−4016.

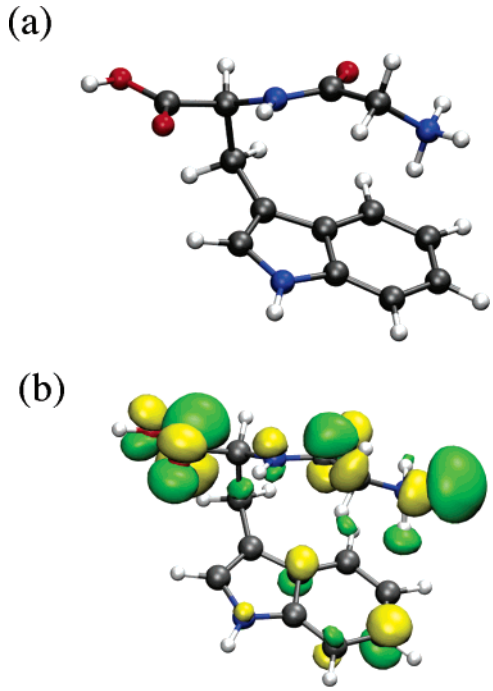

Figure 4. H^+GlyTrp (a) calculated lowest energy configuration, demonstrating the proximity of the ammonium group to the indole ring; (b) dominant Kohn−Sham orbital contributions to the electronic excited state. Note the substantial amount of σ^*_{N-H} character.

NH_3 group (Figure 3c), in agreement with one of the major fragmentation channels that we observe. After a first drop of the excited-state energy, the gap between the ground and the occupied excited state remains approximately constant. The shape of potential energy surfaces (both in the ground and excited states) obtained by RI-CC2 calculations (also shown in Figure 3), as well as the symmetry of the main molecular orbital contribution to the excited state, is in good agreement with the TDDFT data (see Supporting Information). This confirms that the TDDFT dynamics on the excited state is qualitatively and quantitatively correct and that the two π_{CO}^* charge transfer states are indeed spectator states that do not affect the dynamics on the first optically accessible state.[36] NH_3 fragmentation is associated with the excitation of an electron into antibonding σ^* states and concomitant localization of the positive charge on the aromatic ring, which is more favorable in the case of the Trp side chain as compared to Tyr and Phe, due primarily to their difference in ionization potentials.[14]

The presence of two water molecules hydrogen-bonded to the amino group alters considerably the electronic structure of the low-energy excited states of $TrpH^+$. The transitions to σ^*_{N-H} orbitals are shifted up by ~1.3 eV because of their interaction with the lone-pair electrons of the two H_2O molecules, an effect that has been described for other H-bonded systems and that can be rationalized in terms of electrostatic and charge transfer interactions between Lewis type acid−base pairs.[43] As a result, the first photoaccessible state of $TrpH^+(H_2O)_2$ populates what is primarily a π^* orbital. Also, in this case, the shape of the populated orbital is consistent with RI-CC2 calculations. Because of the solvent-induced separation of the π^* state from the dissociative σ^*_{C-N} and σ^*_{N-H} manifold, TDDFT-MD performed on this state does not lead to any appreciable

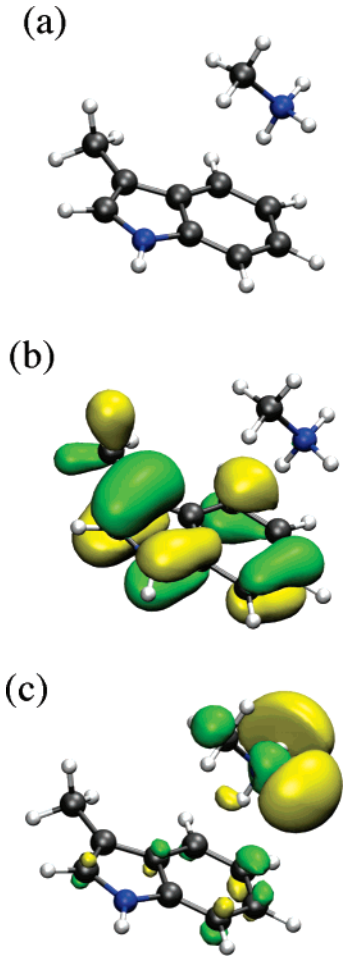

Figure 5. 3-Methylindole−methylammonium complex. (a) Reduced model derived from the H^+GlyTrp dipetide geometry; (b) ground electronic state orbital (HOMO); (c) excited electronic state orbital (LUMO). Note that the HOMO−LUMO transition has ΔE and oscillator strength similar to that of $\pi\sigma^*$ in bare $TrpH^+$ as well as in H^+GlyTrp.

relaxation of the electronic structure, and unlike the case of bare $TrpH^+$, we do not observe any fast covalent fragmentation channel (Figure 3e and f). Instead, the initial release of energy after vertical excitation eventually leads to water dissociation, as observed experimentally.

Our calculations also provide insight into why the dramatic lifetime lengthening occurs with two water molecules rather than one. The structure of $TrpH^+(H_2O)_2$ shown in Figure 2c reveals an intramolecular hydrogen bonding interaction between the nonsolvated ammonium NH bond and the carbonyl oxygen on the amino acid backbone. Thus, with two water molecules, all three of the ammonium NH bonds are involved in hydrogen bonds, which pushes up the energies of the σ^*_{N-H} state that is dissociative in the corresponding coordinate. This can be also seen in the electron density plot of Figure 3d, which shows no σ^*_{N-H} character.

We believe that these effects are not limited to isolated protonated tryptophan but will also be important in tryptophan within proteins whenever positively charged groups are situated nearby. This raises the question of whether the photoinduced charge transfer from the indole ring to the dissociative $\pi\sigma^*$ state on the charged ammonium group is a "through-bond" or "through-space" effect, since in the former case it might only be important in proteins with a charged N-terminal tryptophan.

(43) Umeyama, H.; Morokuma, K. *J. Am. Chem. Soc.* **1977**, *99*, 1316−1332.

To test this, we have performed experiments on H^+GlyTrp and H^+GlyGlyTrp as well as calculations on the former. The ammonium group, which is attached to the N-terminal glycine in each case, is further away from the indole chromophore of tryptophan in terms of the number of bonds between them but is closer in space because of the greater flexibility of the backbone (e.g., Figure 4a). Electronic spectra of these species show no sharp structure, exhibiting linewidths similar to that of bare $TrpH^+$. Moreover, TDDFT calculations on H^+GlyTrp show that the excited state has a strong component of dissociative σ^*_{N-H} character centered on the charged ammonium (Figure 4b).

As a final test of the importance of bond connectivity, we have performed calculations of the excited state of a 3-methylindole−methylammonium complex (Figure 5) in which the geometry is fixed to that calculated for the H^+GlyTrp dipeptide but the ammonium is not covalently linked to the indole ring. In this case, we find that the excited state has significant σ^*_{N-H} character centered on the charged ammonium. Thus, we expect that the effect of charge in shortening the excited-state lifetime is not limited to isolated $TrpH^+$ but should be a general feature of tryptophan embedded in proteins whenever positively charged groups are in close proximity.

Conclusions

Our studies demonstrate that a protonated ammonium group in close proximity to the indole chromophore induces the broadening of the absorption peak of bare $TrpH^+$ and tryptophan-containing peptides. The presence of the charge lowers the energy of the $\pi\sigma^*$ manifold, bringing it in close proximity to the indole $\pi\pi^*$ state, facilitating mixing between them. It is this mixed state with variable σ^* and π^* contributions that plays the key role in tuning the optical properties of the indole chromophore by opening fast dissociative channels.[14,40] Hydration of the NH_3^+ group by as few as two water molecules shifts the σ^*_{N-H} antibonding component to higher energy, decoupling it from the π^* state and hence from the $\pi\pi^*$ transition. As a result, photoexcitation leads to a longer-lived excited state, which, in turn, yields highly resolved spectra.

This combined experimental and theoretical study should have important implications for the interpretation of tryptophan fluorescence data used to probe protein structure and dynamics. For example, recent studies of human serum albumin (HSA) used fluorescence from the Trp214 residue, which is buried inside a deep crevice of the protein, to probe its structure,[44] solvation dynamics, and local rigidity.[45] Site-directed mutagenesis studies[44] have revealed that the presence of a charged arginine residue (Arg218) in the vicinity of Trp214 clearly plays a role in determining its fluorescence lifetime. Our results suggest that the charge on the Arg218 should give rise to low lying states with σ^* character and that electron transfer to this side chain will provide a nonradiative decay path that competes with tryptophan fluorescence. Moreover, the presence of water molecules in the pocket[45] can modify the effect of the arginine charge depending upon their location. Our experimental and theoretical study on a well-defined, gas-phase system begins to provide a molecular level understanding of such effects in proteins.

Acknowledgment. Funding was generously provided by the École Polytechnique Fédérale de Lausanne and the Fonds National Suisse (Grant Nos. 200020-103666/1 and 200020-108063/1). The calculations were performed on the IBM BlueGene/L machine at the EPFL.

Supporting Information Available: Figure showing the orbital character calculated both by TDDFT and RI-CC2 for the populated excited state along the molecular dynamics run taken at the first three time frames labeled with circles in Figure 3b. This material is available free of charge via the Internet at http://pubs.acs.org.

JA065980N

(44) Siemiarczuk, A.; Petersen, C. E.; Ha, C. E.; Yang, J. S.; Bhagavan, N. V. *Cell Biochem. Biophys.* **2004**, *40*, 115−122.
(45) Qiu, W. H.; Zhang, L. Y.; Okobiah, O.; Yang, Y.; Wang, L. J.; Zhong, D. P.; Zewail, A. H. *J. Phys. Chem. B* **2006**, *110*, 10540−10549.